Article:
Zhai, X, Shi, J, Zou, X et al. (6 more authors) (2017) Novel colorimetric films based on starch/polyvinyl alcohol incorporated with roselle anthocyanins for fish freshness monitoring. Food Hydrocolloids, 69. pp. 308-317. ISSN 0268-005X

https://doi.org/10.1016/j.foodhyd.2017.02.014

Accepted Manuscript

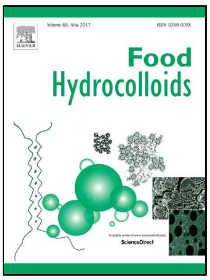

Novel colorimetric films based on starch/polyvinyl alcohol incorporated with roselle anthocyanins for fish freshness monitoring

Xiaodong Zhai, Jiyong Shi, Xiaobo Zou, Sheng Wang, Caiping Jiang, junjun Zhang, Xiaowei Huang, Wen Zhang, Mel Holmes

PII:	S0268-005X(16)30955-9
DOI:	10.1016/j.foodhyd.2017.02.014
Reference:	FOOHYD 3804
To appear in:	*Food Hydrocolloids*
Received Date:	05 December 2016
Revised Date:	20 February 2017
Accepted Date:	20 February 2017

Please cite this article as: Xiaodong Zhai, Jiyong Shi, Xiaobo Zou, Sheng Wang, Caiping Jiang, junjun Zhang, Xiaowei Huang, Wen Zhang, Mel Holmes, Novel colorimetric films based on starch /polyvinyl alcohol incorporated with roselle anthocyanins for fish freshness monitoring, *Food Hydrocolloids* (2017), doi: 10.1016/j.foodhyd.2017.02.014

Graphical abstract

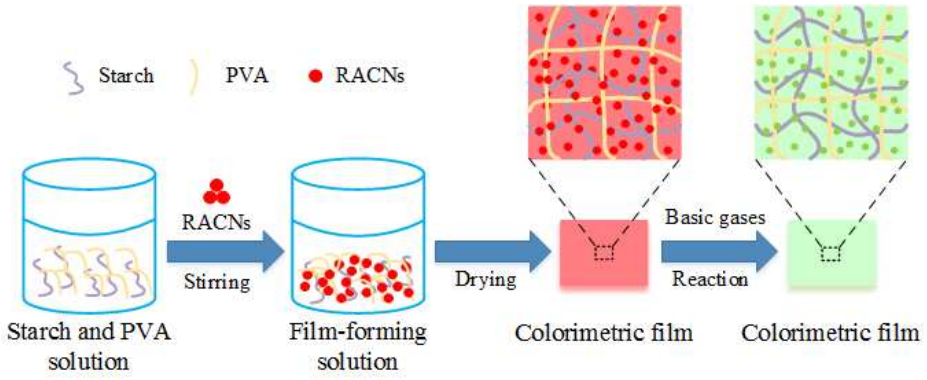

Highlights

- Colorimetric films were developed by using roselle anthocyanins, starch and PVA.
- Roselle anthocyanins improved the compatibility between starch and PVA.
- The colorimetric films had good color stabilities within 14 days at 4℃ and 25℃.
- The colorimetric film with fewer roselle anthocyanins was more sensitive to NH_3.
- The colorimetric films can be used to monitor the fish freshness at 4℃.

Novel colorimetric films based on starch/polyvinyl alcohol incorporated with roselle anthocyanins for fish freshness monitoring

Xiaodong Zhai[#1], Jiyong Shi[#1], Xiaobo Zou[#*1], Sheng Wang[1], Caiping Jiang[1], junjun Zhang[1], Xiaowei Huang[1], Wen Zhang[1], Mel Holmes[2]

[1] Agricultural Product Processing and Storage Lab, School of Food and Biological Engineering, Jiangsu University, Zhenjiang, Jiangsu 212013, China

[2] School of Food Science and Nutrition, the University of Leeds, Leeds LS2 9JT, United Kingdom

[#] These authors contributed equally to this study

[*] Corresponding author. Tel.: +86 511 88780174; fax: +86 511 88780201. Email: zou_xiaobo@ujs.edu.cn

Abstract

Novel colorimetric films were developed for real-time monitoring of fish freshness based on starch/polyvinyl alcohol (SPVA) incorporated with roselle (*Hibiseus sabdariffa* L.) anthocyanins (RACNs). Firstly, RACNs were extracted from roselle dehydrated calyxes. Secondly, SPVA aqueous solution was obtained with a mass rate of 2:1 (starch/PVA). Thirdly, the colorimetric films were fabricated by immobilizing 30, 60 and 120 mg RACNs/100 g starch into SPVA matrix with casting/solvent evaporation method. FTIR spectra of the colorimetric films showed that RACNs were successfully immobilized into the SPVA matrix. X-ray diffraction spectra and SEM micrographs indicated that the crystallinity of PVA was reduced during the film-forming process and the compatibility between starch and PVA was improved, owing to the presence of RACNs. The incorporation of RACNs led to a decrease of water content and tensile strength and an increase of elongation at break of the colorimetric films compared with the SPVA film. The color stability test showed that the colorimetric films were stable at refrigeration temperature and room temperature up to 14 days with relative color changes below than 5%. The colorimetric films with lower content of RACNs were found more sensitive towards ammonia. An application trial was conducted to monitor the freshness of silver carp (*Hypophthalmichthys molitrix*) at refrigeration temperature. The colorimetric films presented visible color changes over time due to a variety of basic volatile amines known as total volatile basic nitrogen (TVB-N). Hence, these colorimetric films can be used to monitor the real-time fish freshness for intelligent packaging.

Keywords: Colorimetric film; Fish freshness; Roselle anthocyanins; Starch; Polyvinyl alcohol; Intelligent packaging.

1. Introduction

Fish is highly perishable due to enzymatic reaction and microbial contamination (Zhang, Sun, Xiao, Liu, & Zheng, 2016). Considering the food quality and safety, it is essential to evaluate the fish freshness during the supply chain. TVB-N has been widely regarded as an useful indicator of the fish freshness for a long period (Olafsdóttir, et al., 1997). It is comprised of ammonia (NH_3), trimethylamine (TMA) and dimethylamine (DMA) generated by the enzymatic decomposition of trimethylamine oxide (TMAO) (Byrne, Lau, & Diamond, 2002). A variety of approaches have been developed to determine the TVB-N level. Chemical methods such as Kjeldahl method can provide precise results, but they are generally time consuming and destructive to samples. Other rapid and non-destructive detection methods, such as FTIR spectroscopy, can also provide satisfactory results (Cai, Chen, Wan, & Zhao, 2011), whereas they need advanced instruments and highly skilled operators. Consequently, these methods are not suitable for consumers to evaluate the real-time freshness.

In the last decades, there was a rapidly growing interest in developing intelligent packaging systems for 'on-package' tracing the real-time food quality. Particularly, colorimetric indicators have received wide attentions because they can exhibit straightforward information by visible color changes. As regard to evaluating the fish freshness, Pacquit, et al. (2007) developed a colorimetric indicator by spin-coating bromocresol green onto a PET substrate. The color of the indicator gradually changed from yellow to green in response to the increasing TVB-N level at room temperature. Similarly, polyaniline-based colorimetric indicator has also been demonstrated to detect the fish spoilage (Kuswandi, et al., 2012). These colorimetric indicators fixed in the headspace of the packaged fish presented specific color changes upon reaction with the TVB-N in the form of gas sensors. In this way, these intelligent packaging systems had great potential to indicate the real-time fish freshness.

Recently, more researches have focused on the natural pigments as a source of color agents, because they are safer and more eco-friendly as compared to chemosynthetic dyes. Anthocyanins are natural water-soluble pigments that have wide

response ranges to pH variation. Several kinds of anthocyanins have been utilized to fabricate the colorimetric indicators for sensing the food quality, such as anthocyanins extracted from red cabbage (Pereira, de Arruda, & Stefani, 2015), grape skin (Ma & Wang, 2016) and purple sweet potato (Choi, Lee, Lacroix, & Han, 2017). Zhang, Lu, and Chen (2014) developed a pH sensing film by incorporating anthocyanins extracted from *Bauhinia blakeana Dunn* with chitosan and the pH sensing film presented a distinguishable color change from purple to green due to the basic volatile gases generated from the fish, suggesting that the anthocyanins-based colorimetric films were good candidates of gas sensors for monitoring fish freshness. When a constant amount of fish samples was stored in a specific circumstance (e.g. temperature, packaging volume), the concentration of the TVB-N in the headspace was definite after a specific period of storage. Therefore, the extent of color change of the colorimetric film was related to the content of the anthocyanins. However, the effect of the anthocyanins content on color rendering properties of the colorimetric film has not been investigated yet.

Roselle (*Hibiseus sabdariffa* L.) is an herbaceous plant, cultivated largely in tropical and subtropical areas of both hemispheres (Sinela, et al., 2017). Its calyxes contain high amounts of anthocyanins up to 1.5 g/100 g on dry weight basis (Degenhardt, Knapp, & Winterhalter, 2000). The biological activities of roselle anthocyanin (RACNs), such as antioxidant activity (Tsai, McIntosh, Pearce, Camden, & Jordan, 2002) and anti-hypertensive effect (Ajay, Chai, Mustafa, Gilani, & Mustafa, 2007) have been widely studied, while the potential use of RACNs for the development of colorimetric indicators has not been explored. In order to immobilize the anthocyanins, several natural polymers have been used for making different colorimetric films, including chitosan (Zhang, et al., 2014), starch (Choi, et al., 2017; Golasz, Silva, & Silva, 2013) and cellulose (Ma, et al., 2016). Among them, starch has received greater attention because of its stability to heat, acid and base conditions. However, pure starch film generally lacks the strength and processability, which can be alternatively addressed by adding polyvinyl alcohol (PVA) (Sin, Rahman, Rahmat, & Mokhtar, 2011). Since 1980s, starch/polyvinyl alcohol (SPVA) films have been studied

for packaging applications (Tang, Zou, Xiong, & Tang, 2008; Tang & Alavi, 2011). They have good transparency (Cano, Cháfer, Chiralt, & González-Martínez, 2015), which is beneficial for the development of colorimetric films. Furthermore, starch and PVA are both non-toxic, renewable and biodegradable (Lu, Xiao, & Xu, 2009; Rezaei, Nasirpour, & Fathi, 2015), which can eliminate the public concerns over food safety and environmental problems.

Therefore, in this study, we aimed to develop new colorimetric films by incorporating various content of RACNs into SPVA matrix through casting/solvent evaporation method. The microstructure of colorimetric films was studied by using X-ray diffractometer and SEM. The effect of the RACNs content on mechanical properties, color stability and sensitivity toward ammonia of the colorimetric films was investigated. Finally, the colorimetric films were employed to monitor the freshness of silver carp (*Hypophthalmichthys molitrix*) at refrigeration temperature (4℃).

2. Material and methods

2.1. Materials

Roselle dehydrated calyxes and live silver carp were obtained from the local market in Zhenjiang, China. Other materials including soluble starch, polyvinyl alcohol (MW: 1750 ± 50), ethyl alcohol (C_2H_6O), potassium chloride (KCl), sodium acetate ($CH_3COONa{\cdot}3H_2O$), magnesium oxide (MgO), methyl red ($C_{15}H_{15}N_3O_2$), methylene blue ($C_{16}H_{18}ClN_3S$), boric acid (H_3BO_3), ammonia solution ($NH_3{\cdot}H_2O$, 25%~27%), acetic acid (CH_3COOH) and hydrochloric acid (HCl) were all purchased from Sinopharm Chemical Reagent Co., Ltd (Shanghai, China). Plastic Petri dishes were purchased from Sigma Chemical Co. (St. Louis, MO, USA).

2.2. Extraction of anthocyanins from roselle dehydrated calyxes

The anthocyanins were extracted according to Chang, et al. (2012) with a slight modification. The roselle dehydrated calyxes were crushed and blended with 75% ethanol aqueous solution at a solid–liquid ratio of 1:10 for 2 h at 25℃. The extract was centrifuged at 8000 rpm for 20 min. The extraction procedure was repeated three times.

Ethanol in filtrate was removed with a rotary evaporator at 35℃ in dark. Finally, the solution was freeze-dried under vacuum and the obtained anthocyanins extract powder was stored in sample vials at 4℃ in the nitrogen atmosphere.

2.3. Determination of total anthocyanins content in extract powder

The anthocyanins content in extract powder was measured by pH differential method (Wang, Li, Chen, Xin, & Yuan, 2013) using a UV-Vis spectrophotometry (Agilent CARY 100, Varian Corporation, USA). The anthocyanins extract powder (20 mg) was dissolved in 10 mL distilled water, and 1 mL anthocyanins solution was dissolved in 9 mL of 0.025 M potassium chloride buffer (pH 1.0) and 9 mL of 0.4 M sodium acetate buffer (pH 4.5) respectively in separate test tubes. Absorbance of sample was measured at 520 and 700 nm. The anthocyanins content was expressed in mg/g.

2.4. Preparation of the colorimetric films

Firstly, 100 mL aqueous dispersion containing 2 g starch and 1 g PVA was heated at 100℃ in a water bath and stirred with a magnetic stirrer until it was completely dissolved. Based on the calculated anthocyanins content (9.51 ± 0.41 mg/g) (refer to section 2.3), a certain amount of anthocyanins extract powder was then added to the cooled SPVA solution at 30, 60 and 120 mg RACNs/100 g starch, expressed as RACNs-30, RACNs-60 and RACNs-120, respectively. The mixtures were then homogenized (Ultra Turrax IKA T25 digital, Germany) at 8000 rpm for 5 min and degassed with a sonicator (Branson CPX5800H, USA) for 5 min at room temperature. Each film was prepared by casting 10 mL of the film-forming solution into a clean and smooth plastic Petri dish with a 53 mm diameter. The Petri dishes were placed on a level surface in an incubator at 35℃ with 50% RH for 36 h. After that, the films were peeled from the Petri dishes and stored at 4℃ with 75% RH for further use.

2.5. Spectral characteristic of RACNs

The color and spectra of RACNs solution at different pH (2-12) were recorded using a UV-Vis Spectrophotometer (Agilent CARY 100, Varian Corporation, USA) in

155 the range of 400-800 nm.

156 2.6. Characterization of the colorimetric films

157 2.6.1. FTIR spectroscopy

158 Fourier transform infrared (FTIR) spectra of the films were determined with a
159 FTIR spectrometer (Perkine Elmer 16 PC spectrometer, Boston, USA). Spectra were
160 recorded at the absorbance mode from 4000 to 650 cm^{-1} at a resolution of 4 cm^{-1} and
161 the total number of scans was 32. OMNIC Spectra software (Thermo Scientific Co.,
162 USA) was used to configure the FTIR spectrometer for scanning and mathematical
163 processing.

164 2.6.2. X-ray diffraction spectra

165 X-ray diffraction (XRD) spectra of films were measured using an X-ray
166 diffractometer (D8 ADVANCE, Bruker, Germany) with a reference of target of Cu Ka
167 radiation, voltage of 40 kV, current of 30 mA. The films were measured at an angle
168 from 5° to 40° (2θ) with steps of 2° (2θ)/min.

169 2.6.3. Scanning electron microscopy (SEM)

170 The micrographs of the films were recorded by a field emission scanning electron
171 microscopy (FE-SEM) (S-4800, Hitachi High-Technologies corporation, Japan). The
172 films were first freeze-fractured by liquid nitrogen before measurement. Samples were
173 attached to double-sided adhesive tape and mounted on the specimen holder, then
174 sputtered and coated with gold under vacuum.

175 2.6.4. Thickness, water content and mechanical properties of the films

176 The thickness of the films was measured by a hand-held digital micrometer
177 (Sanfeng Group Co., Ltd., Taiwan, China). The thickness was measured at 20 random
178 positions on the films.

179 To determine the moisture content (MC), the films were dried to an equilibrium
180 weight at 105℃ in an oven. MC was calculated according to the following equation:

$$MC(\%) = 100 \times \left(M_i - M_f \right) / M_i \quad (1)$$

where M_i was the initial weight of films stored in 75% RH to moisture equilibrium (g) and M_f was the final weight of films dried at 105℃ (g).

Tensile strength (TS) and elongation at break (EB) were measured with an Instron Universal Testing Machine (Model 4500, Instron Corporation, Canton, MA, USA) using a modified ASTM D882-00 (ASTM, 2000b) procedure. Each film was cut in rectangular strips with 40 mm length and 20 mm width. The initial grip separation and crosshead speed were set at 20 mm and 0.6 mm/s, respectively. Measurements represent an average of three samples. The TS and EB were calculated as the following equations:

$$TS = F_{\max} / S \quad (2)$$

$$EB = 100 \times \Delta l / l_0 \quad (3)$$

where TS was the tensile strength (MPa); $F_{\max}$ was the maximun load (N); S was the initial cross-sectional area of the film sample (mm^2); EB was the elongation at break; Δl was the extension of the films (mm) and l_0 was the intial length of the films (20 mm).

2.6.5. Color stability of the colorimetric films

The colorimetric films were stored in incubators at 4℃ and 25℃ with 75% RH under fluorescent lights. The images of the colorimetric films were captured every day for two weeks by an optical scanner (Scanjet G4050, HP) and analyzed by a user program in Matlab R2012a (Matworks Inc., Natick, MA, USA). The stability of the colorimetric films was difined as the relative color change (Xiaowei, et al., 2015):

$$\Delta R = \left| R_0 - R_1 \right| \quad (4)$$

$$\Delta G = \left| G_0 - G_1 \right| \quad (5)$$

$$\Delta B = \left| B_0 - B_1 \right| \quad (6)$$

$$S = \frac{\Delta R + \Delta G + \Delta B}{R_0 + G_0 + B_0} \times 100\% \quad (7)$$

where R_0, G_0, B_0 were the initial gray values of the red, green and blue, R_1, G_1, B_1 were the gray values of the red, green and blue after storage. S was the relative color change

of *R*, *G* and *B* values.

2.6.6. Response of the colorimetric films to ammonia

Response of the colorimetric films toward volatile ammonia in term of their color changes was performed using absorbance measurements (Kuswandi, et al., 2012). The colorimetric films were cut into squares (10 × 10 mm) and hang up in an erlenmeyer flask (500 mL) at 1 cm above the ammonia solution (80 mL, 8 mM) for 24 min at 25℃. UV-vis spectra of the films in the range of 400-800 nm were recorded every 2 min by a hand-held fiber optical vis-NIR spectrometer (Ocean Optics Co., ltd, USA).

2.7. Application of the colorimetric films for monitoring fish freshness

2.7.1. Fish spoilage trial

Live silver carp was cut into strips after removing its innards, head, tail and feathers. Then, 20 g of silver carp was immediately transferred into covered Petri dishes with 90 mm diameters. The colorimetric films were placed in the headspace of the Petri dish. The Petri dishes were stored in a refrigerator at 4℃ for 165 h. The color of the colorimetric films was recorded after every 15 h by using the optical scanner.

2.7.2. Determination of TVB-N

The TVB-N level of the fish sample was measured by a stream distillation method (Cai, et al., 2011). The 10 g portion was placed in a beaker, blended with 100 mL distilled water, then grounded by using a tissue homogenizer (A-88, Jintan medical instrument plant, China). The homogenate was filtered by using filter papers. Then, 5.0 mL filtrare was transfered to Kjeldahl distillation unit (ZLQ03, East China Glass Co. Ltd., China) with addition of 5 mL 1% magnesium oxide suspension (1 g/L). The distillate was collected in a flask containing 10 mL 2% aqueous solution of boric acid and 3 droplets of mixed indicator produced from dissolution of 0.2 g of methyl red and 0.1 g of methylene blue to 100 mL of ethanol. After that, the boric acid solution was titrated with a 0.01 M hydrochloric acid solution. TVB-N value was determined by the hydrochloric acid used during titration.

3. Results and discussion

3.1. Color and spectral properties of RACNs

Fig. 1a shows the color change of RACNs solutions in the pH range of 2 to 12. It can be seen that the color of RACNs solutions was pink at pH lower than 5, and changed gradually to purple at pH 6-7. When the solutions were basic, the color altered to blue and yellow at pH 8-9 and 10-12, respectively. The UV-vis spectra of RACNs solutions corresponding with color changes were recorded, as shown in Fig. 1b. When the pH value was lower than 4, the maximum absorption peak was obtained at 520 nm and the absorbance gradually decreased with the increase of pH value. As the pH increased from 5 to 8, the maximum absorption peak showed a bathochromic shift from 540 to 580 nm, accompanied with an increase of maximum absorbance. Furthermore, the absorbance at 580 nm decreased with the increase of pH in the range of 8-12.

The color variation and the corresponding peak shift was originated by their structure transformation (Castañeda-Ovando, Pacheco-Hernández, Páez-Hernández, Rodríguez, & Galán-Vidal, 2009). Different anthocyanins generally demonstrate different color response to pH variation (Garber, Odendaal, & Carlson, 2013). Herein, the color response of the crude RACNs extract solution was an integrated color response of several kind of anthocyanins, mainly including delphinidin-3-sambubioside and cyanidin-3-O-sambubioside (Grajeda-Iglesias, et al., 2016).

Fig. 1

3.2. Characterization of the colorimetric films

3.2.1. FTIR analysis

Fig. 2 shows FTIR spectra of the starch, PVA, RACNs, SPVA film and the colorimetric films. In the spectrum of starch, the broad band at 3289 cm^{-1} and the peak at 1639 cm^{-1} were attributed to the stretching vibration and bending vibration of O-H, respectively. The peak at 2924 cm^{-1} corresponded to bending vibration of C-H. The characteristic peak occurred at 1639 cm^{-1} was the feature of tightly bound water present in starch. The bands from 761 to 1077 cm^{-1} corresponded to the C-O bond stretching

(Xu, Kim, Hanna, & Nag, 2005). The spectrum for PVA showed the maximum absorption peak at 1086 cm^{-1} resulting from the C-O bond stretching and the peak at 1416 cm^{-1} corresponding to bending vibration of $CH\text{-}CH_2$ certified the basic carbon skeleton of PVA (Pereira, et al., 2015). In terms of RACNs spectrum, the peaks between 2800-3300 cm^{-1}, and the peaks at 1709 and 923 cm^{-1} were the three characteristic bands for the recognition of carboxyl group, assigned to the stretching vibration of O-H and C=O, and the out-of-plane bending vibration of -OH, respectively. The peak at 1596 cm^{-1} was related to the combinations and overtones of aromatic compounds (Pereira, et al., 2015). The anthocyanins spectrum showed the maximum absorption peak at 1023 cm^{-1}, corresponding to aromatic ring C-H deformation. No significant difference between the spectra of colorimetric films could be observed. However, compared with the spectrum of SPVA film, a new peak around 1627 cm^{-1} which was related to the combinations and overtones of aromatic compounds appeared in the spectra of the colorimetric films, certifying that RACNs have been incorporated into the starch/PVA matrix.

Fig. 2

3.2.2. XRD analysis

For starch granules, there are usually A, B, and C-type by XRD spectra because of their different crystalline structures (Buléon, Colonna, Planchot, & Ball, 1998; Tian, Rickard, & Blanshard, 1991). A-type starch has strong diffraction peaks at about 15° and 23° and unresolved doublet at around 17° and 18°, while B-type starch possess the strongest diffraction peak at around 17°, some small peaks at around 15°, 20°, 22° and 24°, and a characteristic peak at about 5.6° (Guo, Liu, Lian, Li, & Wu, 2014). C-type starch is a mixture of A and B-type starch. As shown in Fig. 3, the starch showed the strongest diffraction peaks at 17.1°, and weak peaks at 15.1°, 19.8°, 22.2° and 24.1°. The weakest characteristic peak at 5.7° was also observed. The results indicated that the starch granules were B-type. In the diffractogram of PVA, the peaks at around 11.6°, 19.4°, 23.0° and the small hump at around 40.8° were associated to its crystalline structure (Sreekumar, Al-Harthi, & De, 2012).

As to the X-ray diffraction of SPVA film, no characteristic peak of starch granule appeared, which indicated that starch was well-dispersed in the SPVA film without crystalline structure, because the crystalline regions of starch granules were destroyed by heating and mechanical stirring during gelatinization. The broad peak in the range of 10-17° resulted from the amorphous state of starch in the SPVA film. However, there was a characteristic peak of PVA at 19.4°, indicating that there was partial crystal structure of PVA remained during the film-forming process. As regarded to the colorimetric films, the peak areas at 19.4° were smaller than that of SPVA film, and decreased with the increase of RACNs content. This indicated that there were fewer rearrangement of PVA molecules to crystallization. This phenomenon was probably due to the hydrogen bond formed between hydroxyl groups of anthocyanins and PVA. The dispersed phase of PVA molecules would be beneficial for the uniformity of films.

Fig. 3

3.2.3. SEM micrographs analysis

The cross-section of the SPVA film and colorimetric films are shown in Fig. 4. It could be observed that the SPVA film showed a two-phase structure. The continuous phase on the left was the starch-rich phase, while the network-like phase on the right was the PVA-rich phase. This structure was due to a certain degree of immiscibility between starch and PVA, which was also observed in a previous research (Cano, Cháfer, Chiralt, & González-Martínez, 2015). However, when RACNs were incorporated into the SPVA film, the cross-section of colorimetric films became homogeneous without phase separation. This implied that RACNs had excellent compatibility with SPVA, and simultaneously improved the compatibility between starch and PVA. Generally, the compatibility of starch and PVA can be improved by adding plasticizers such as glycerol, sorbitol, poly(ethylene glycol) and monosaccharides (Jiang, et al., 2012). These plasticizers contain a number of hydroxyl groups that can form intermolecular hydrogen bonds with the hydroxyl groups of starch and PVA and thus reduce the intermolecular hydrogen bonds and entanglements between polymer chains (Jiang, et al., 2012). In this work, the enhanced compatibility

between starch and PVA may also be ascribed to the hydrogen bonds between the hydroxyl groups of RACNs, starch and PVA. Furthermore, the cross-sections of the colorimetric films became more compact as a result of an increasing content of RACNs, indicating the more intensive interactions.

Fig. 4

3.2.4. Thickness, water content and mechanical properties of the films

Table 1 shows the thickness, water content and the mechanical properties of the SPVA film and the colorimetric films. The SPVA/RACNs-120 film had the highest thickness, and no significant difference was observed between the thicknesses of the SPVA film, SPVA/RACNs-30 film and SPVA/RACNs-60 film. The water content (*WC*) of SPVA/RACNs-30 film was close to the SPVA film. However, when the RACNs content was higher than 60 mg/100 g starch, the *WC* of films significantly decreased with the increase of RACNs content. This was probably because the interaction between SPVA and RACNs could lower the availability of hydroxyl groups of SPVA, which would in turn limit the SPVA-water interactions (Wang, Dong, Men, Tong, & Zhou, 2013). The content of RACNs also had significant effect on the mechanical properties of the films. As can be seen, the tensile strength (*TS*) decreased with RACNs addition increasing from 30 to 120 mg/100 g starch, while the elongation at break (*EB*) increased with the increase of RACNS content. A similar behavior was found in SPVA films incorporated with hydroxyl group-riched glycerol (Yoon, Chough, & Park, 2006). The decrease of *TS* could be due to that the intramolecular interaction of starch molecules and PVA molecules was interrupted by the RACNs molecules, whereas the increase of *EB* was because the RACNs improved the compatibility of starch and PVA so that the films became more homogeneous, as shown in section 3.2.3, which resulted in enhanced extensibility.

Table 1

3.2.5. Color stabilities of the colorimetric films

The self-stabilities of the colorimetric films were essential to their color

348 performance. Fig. 5 shows the relative color changes (*S*) of the colorimetric films. It
349 can be seen that the colorimetric films stored at 4℃ had small *S* values which were
350 lower than 1% within 14 days, showing that they had excellent color stabilities. There
351 was no obvious difference between the *S* values of the colorimetric films with different
352 content of RACNs. By contrast, the colorimetric films had higher *S* values when they
353 were stored at 25℃. Obvious increase of *S* values can be observed in the first day, which
354 may be due to the moisture equilibrium process of the colorimetric films with the
355 surrounding environment. After that, the *S* values gradually increased with time, this
356 was owing to that RACNs were partially oxidized by the oxygen. Furthermore, the *S*
357 values of the colorimetric films decreased with the increase of RACNs content,
358 indicating that the colorimetric films with more RACNs possessed greater color
359 stabilities. Nevertheless, the *S* values were overall lower than 5%, implying that the
360 colorimetric films had great color stabilities at 25℃ as well.

361 Generally, the isolated anthocyanins are highly unstable and their stabilities are
362 affected by several factors such as pH, storage temperature, chemical structure, light,
363 oxygen, and their concentration (Castañeda-Ovando, et al., 2009). The color stability
364 of RACNs solution stored at different temperatures has been studied by Sinela, et al.
365 (2017) who found that the RACNs solution had great stability at 4℃. Apart from the
366 storage temperature, in this work, the great color stabilities of the colorimetric films
367 may be, on one hand, owing to the low water content of the colorimetric films that
368 reduced the hydration of anthocyanins thus preserving the color (Lewis, Walker, &
369 Lancaster, 1995). On the other hand, starch and PVA may protect the anthocyanins
370 from being oxidized to some extent by entrapping the anthocyanins. Moreover, the
371 RACNs incorporated into the colorimetric films were crude extract, in which the co-
372 pigments such as sugar and phenolic acids could contribute to the color stability of
373 anthocyanins (Sui, Bary, & Zhou, 2016).

374 **Fig. 5**

375 3.2.6. Response of colorimetric films to ammonia vapor

376 In order to find out the response behavior of the colorimetric films towards the

volatile basic gas, the colorimetric films were exposed to the ammonia generated from the 8 mM ammonia solution under 25℃ for 24 min and UV-vis spectra were recorded. The initial maximum absorption peak were all observed at 540 nm for these three colorimetric films as shown in Fig. 6a, b and c, indicating a red shift compared with the RACNs solution (520 nm). Similar red shift was also observed in chitosan films containing bauhinia blakeana dunn anthocyanins (Zhang, et al., 2014). The absorption peak at 540 nm decreased and another absorption peak at 640 nm gradually increased with reaction time. These results indicated that the colorimetric films gradually transferred to be more basic. The absorbance ratio at 640 nm versus 540 nm (A_{640}/A_{540}) represented the green color intensity compared to the red color intensity (Choi, et al., 2017), which increased with time as shown in Fig. 6d. The calibration curves showed that A_{640}/A_{540} increased exponentially with the reaction time as the following formulas, where x was the reaction time and y was A_{640}/A_{540}:

$y = 0.1235e^{0.0644x}, R^2 = 0.992$, for SPVA/RACNs-30 film; （8）

$y = 0.0917e^{0.0611x}, R^2 = 0.9965$, for SPVA/RACNs-60 film; （9）

$y = 0.0505e^{0.0059x}, R^2 = 0.9819$, for SPVA/RACNs-120 film. （10）

The slope of calibration curve represented the rate of color variation from red to green, a greater slope indicated a higher variation rate. At a certain reaction time, the SPVA/RACNs-30 film had the highest color variation rate, followed by the SPVA/RACNs-60 film and then the SPVA/RACNs-120 film. This result indicated that the colorimetric film with fewer RACNs was more sensitive to NH_3. The color variation mechanism of the colorimetric films was that the volatiled NH_3 firstly combained with H_2O contained in the colorimetric film to form $NH_3 \cdot H_2O$ which then hydrolyzed to produce NH_4^+ and OH^-, the latter of which induced the color change of RACNs. The higher color variation rate occored in the colorimetric films with fewer RACNs was due to that the discolored RACNs took higher proportions of the total RACNs within the same reaction time. It was generally expected that gas sensors could have fast response to the analytes. Hence, the SPVA/RACNs-30 film that exhibited the highest color variation rate would contribute to its application as a gas sensor.

406 **Fig. 6**

407 3.3. Trials on monitoring the fish freshness

408 TVB-N level was used as the indicator to determine the fish freshness. As shown
409 in Fig. 7a, the initial TVB-N value of the fresh fish was 6.61 mg/100 g, and then it
410 increased up to 28.53 mg/100 g at 165 h. According to Chinese Standard (GB 2733-
411 2015), the rejection limit of TVB-N level for silver carp is 20 mg/100 g. This implied
412 that the fish sample could not be consumed almost after 135 h.

413 The color changes of the colorimetric films were shown in Fig. 7b. The
414 SPVA/RACNs-30 film presented a purple color at the beginning, then green color at
415 90 h and finally yellow color after 135 h, while the SPVA/RACNs-60 film changed its
416 color from initial pink to purple at 90 h and green after 150 h. As to the SPVA/RACNs-
417 60 film, it showed a red color at first which turned to pink at 105 h and purple after 135
418 h. These color changes indicated that the colorimetric films became more basic due to
419 the increasing TVB-N. However, it can be observed that the SPVA/RACNs-30 film
420 exhibited the highest color change rate, followed by the SPVA/RACNs-60 film and
421 then the SPVA/RACNs-120 film. This was in consist with the results found in 3.2.5
422 section in which the colorimetric films with lower content of RACNs had higher color
423 change rates.

424 All of the colorimetric films displayed continuous color changes within the shelf
425 life of fish (135 h), suggesting that they were capable to indicate the real-time fish
426 freshness. Furthermore, it was well received for the colorimetric films to have rapid
427 response to the TVB-N so that they could indicate the fish freshness in the early stages
428 of storage. From this aspect, the SPVA/RACNs-30 film and SPVA/RACNs-60 film
429 which presented earlier color variation were superior to the SPVA/RACNs-120 film,
430 because the SPVA/RACNs-120 film did not show discriminative color changes until
431 75 h. However, it was worth mentioning that the colors displayed by the
432 SPVA/RACNs-30 film were not deep enough to be easily seen by naked eyes. These
433 results suggested that the colorimetric film with an appropriate content of anthocyanins
434 would be favorable to its practical application for real-time monitoring the fish

freshness. The colorimetric film with a high content of anthocyanins would take a long time for its color shift, while the colorimetric film containing an extremely low content of anthocyanins would present weak colors although it had rapid color changes.

Fig. 7

4. Conclusions

Novel colorimetric films were successfully developed by incorporating 30, 60 and 120 mg RACNs/100 g starch with SPVA through casting/solvent evaporation method. The FTIR spectra of the colorimetric films certified that RACNs were successfully immobilized into the SPVA matrix. X-ray diffraction spectra and SEM micrographs indicated that the crystallinity of PVA was reduced during the film-forming process and the compatibility between starch and PVA was improved, owing to the presence of RACNs. The incorporation of RACNs led to a decrease of water content and tensile strength, and an increase of elongation at break. The color stability test showed that the colorimetric films were stable within 14 days at 4℃ and 25℃. The colorimetric film with lower content of RACNs was more senisitive to ammonia. The results of the application trial showed that the SPVA/RACNs-60 film were able to indicate the real-time fish freshness by visible color changes. All the materials used to fabricate the colorimetric films were nontoxic and biodegradable. Hence, the colorimetric films can be used as safe and eco-friendly fish freshness indicators for intelligent packaging.

Acknowledgment

The authors gratefully acknowledge the financial support provided by the national science and technology support program (2015BAD17B04, 2015BAD19B03), the national natural science foundation of China (Grant No.61301239), China postdoctoral science foundation (2013M540422, 2014T70483, 2016M590422), the national natural science foundation of China (31601543), the natural science foundation of Jiangsu province (BK20160506), science foundation for postdoctoral in Jiangsu province (1301051C), Suzhou science and technology project (SNG201503), international science and technology cooperation project of Zhenjiang (GJ2015010), research foundation for advanced talents in Jiangsu University (13JDG039) and Priority Academic Program Development of Jiangsu Higher Education Institutions (PAPD). We also would like to thank our colleagues in School of Food and Biological Engineering who provided assistance in this study.

Notes

The authors declare no competing financial interest.

Reference

Ajay, M., Chai, H. J., Mustafa, A. M., Gilani, A. H., & Mustafa, M. R. (2007). Mechanisms of the anti-hypertensive effect of Hibiscus sabdariffa L. calyces. *Journal of Ethnopharmacology, 109*(3), 388-393.

Buléon, A., Colonna, P., Planchot, V., & Ball, S. (1998). Starch granules: structure and biosynthesis. *International Journal of Biological Macromolecules, 23*(2), 85-112.

Byrne, L., Lau, K. T., & Diamond, D. (2002). Monitoring of headspace total volatile basic nitrogen from selected fish species using reflectance spectroscopic measurements of pH sensitive films. *The Analyst, 127*(10), 1338-1341.

Cai, J., Chen, Q., Wan, X., & Zhao, J. (2011). Determination of total volatile basic nitrogen (TVB-N) content and Warner–Bratzler shear force (WBSF) in pork using Fourier transform near infrared (FT-NIR) spectroscopy. *Food Chemistry, 126*(3), 1354-1360.

Cano, A., Cháfer, M., Chiralt, A., & González-Martínez, C. (2015). Physical and Antimicrobial Properties of Starch-PVA Blend Films as Affected by the Incorporation of Natural Antimicrobial Agents. *Foods, 5*(1), 3.

Cano, A. I., Cháfer, M., Chiralt, A., & González-Martínez, C. (2015). Physical and microstructural properties of biodegradable films based on pea starch and PVA. *Journal of Food Engineering, 167*, 59-64.

Castañeda-Ovando, A., Pacheco-Hernández, M. d. L., Páez-Hernández, M. E., Rodríguez, J. A., & Galán-Vidal, C. A. (2009). Chemical studies of anthocyanins: A review. *Food Chemistry, 113*(4), 859-871.

Chang, X. L., Wang, D., Chen, B. Y., Feng, Y. M., Wen, S. H., & Zhan, P. Y. (2012). Adsorption and desorption properties of macroporous resins for anthocyanins from the calyx extract of roselle (Hibiscus sabdariffa L.). *Journal of Agricultural and Food Chemistry, 60*(9), 2368-2376.

Choi, I., Lee, J. Y., Lacroix, M., & Han, J. (2017). Intelligent pH indicator film composed of agar/potato starch and anthocyanin extracts from purple sweet potato. *Food Chemistry, 218*, 122-128.

Degenhardt, A., Knapp, H., & Winterhalter, P. (2000). Separation and Purification of Anthocyanins by High-Speed Countercurrent Chromatography and Screening for Antioxidant Activity. *Journal of Agricultural and Food Chemistry, 48*(2), 338-343.

Garber, K. C. A., Odendaal, A. Y., & Carlson, E. E. (2013). Plant Pigment Identification: A Classroom and Outreach Activity. *Journal of Chemical Education, 90*(6), 755-759.

Golasz, L. B., Silva, J. D., & Silva, S. B. D. (2013). Film with anthocyanins as an indicator of chilled pork deterioration. *Ciência E Tecnologia De Alimentos, 33*(2), 155-162.

Grajeda-Iglesias, C., Figueroa-Espinoza, M. C., Barouh, N., Barea, B., Fernandes, A., de Freitas, V., & Salas, E. (2016). Isolation and Characterization of Anthocyanins from Hibiscus sabdariffa Flowers. *Journal of Natural Products, 79*(7), 1709-1718.

Guo, J., Liu, L., Lian, X., Li, L., & Wu, H. (2014). The properties of different cultivars of Jinhai sweet potato starches in China. *International Journal of Biological Macromolecules, 67*, 1-6.

Jiang, X., Jiang, T., Gan, L., Zhang, X., Dai, H., & Zhang, X. (2012). The plasticizing mechanism and effect of calcium chloride on starch/poly(vinyl alcohol) films. *Carbohydrate Polymers, 90*(4), 1677-1684.

Kuswandi, B., Jayus, Restyana, A., Abdullah, A., Heng, L. Y., & Ahmad, M. (2012). A novel colorimetric food package label for fish spoilage based on polyaniline film. *Food Control,*

25(1), 184-189.

Lewis, C. E., Walker, J. R. L., & Lancaster, J. E. (1995). Effect of polysaccharides on the colour of anthocyanins. *Food Chemistry, 54*(3), 315-319.

Lu, D. R., Xiao, C. M., & Xu, S. J. (2009). Starch-based completely biodegradable polymer materials. *Express Polymer Letters, 3*(6), 366-375.

Ma, Q., & Wang, L. (2016). Preparation of a visual pH-sensing film based on tara gum incorporating cellulose and extracts from grape skins. *Sensors and Actuators B: Chemical, 235*, 401-407.

Olafsdóttir, G., Martinsdóttir, E., Oehlenschläger, J., Dalgaard, P., Jensen, B., Undeland, I., Mackie, I. M., Henehan, G., Nielsen, J., & Nilsen, H. (1997). Methods to evaluate fish freshness in research and industry. *Trends in Food Science & Technology, 8*(8), 258-265.

Pacquit, A., Frisby, J., Diamond, D., Lau, K., Farrell, A., Quilty, B., & Diamond, D. (2007). Development of a smart packaging for the monitoring of fish spoilage. *Food Chemistry, 102*(2), 466-470.

Pereira, V. A., de Arruda, I. N. Q., & Stefani, R. (2015). Active chitosan/PVA films with anthocyanins from Brassica oleraceae (Red Cabbage) as Time–Temperature Indicators for application in intelligent food packaging. *Food Hydrocolloids, 43*, 180-188.

Rezaei, A., Nasirpour, A., & Fathi, M. (2015). Application of Cellulosic Nanofibers in Food Science Using Electrospinning and Its Potential Risk. *Comprehensive Reviews in Food Science and Food Safety, 14*(3), 269-284.

Sin, L. T., Rahman, W. A. W. A., Rahmat, A. R., & Mokhtar, M. (2011). Determination of thermal stability and activation energy of polyvinyl alcohol–cassava starch blends. *Carbohydrate Polymers, 83*(1), 303-305.

Sinela, A., Rawat, N., Mertz, C., Achir, N., Fulcrand, H., & Dornier, M. (2017). Anthocyanins degradation during storage of Hibiscus sabdariffa extract and evolution of its degradation products. *Food Chemistry, 214*, 234-241.

Sreekumar, P. A., Al-Harthi, M. A., & De, S. K. (2012). Studies on compatibility of biodegradable starch/polyvinyl alcohol blends. *Polymer Engineering & Science, 52*(10), 2167-2172.

Sui, X., Bary, S., & Zhou, W. (2016). Changes in the color, chemical stability and antioxidant capacity of thermally treated anthocyanin aqueous solution over storage. *Food Chemistry, 192*, 516-524.

Tang, S., Zou, P., Xiong, H., & Tang, H. (2008). Effect of nano-SiO2 on the performance of starch/polyvinyl alcohol blend films. *Carbohydrate Polymers, 72*(3), 521-526.

Tang, X., & Alavi, S. (2011). Recent advances in starch, polyvinyl alcohol based polymer blends, nanocomposites and their biodegradability. *Carbohydrate Polymers, 85*(1), 7-16.

Tian, S. J., Rickard, J. E., & Blanshard, J. M. V. (1991). Physicochemical properties of sweet potato starch. *Journal of the Science of Food and Agriculture, 57*(4), 459-491.

Tsai, P.-J., McIntosh, J., Pearce, P., Camden, B., & Jordan, B. R. (2002). Anthocyanin and antioxidant capacity in Roselle (Hibiscus Sabdariffa L.) extract. *Food Research International, 35*(4), 351-356.

Wang, L., Dong, Y., Men, H., Tong, J., & Zhou, J. (2013). Preparation and characterization of active films based on chitosan incorporated tea polyphenols. *Food Hydrocolloids, 32*(1), 35-41.

Wang, Z., Li, Y., Chen, L., Xin, X., & Yuan, Q. (2013). A study of controlled uptake and release of anthocyanins by oxidized starch microgels. *Journal of Agricultural and Food Chemistry, 61*(24), 5880-5887.

Xiaowei, H., Xiaobo, Z., Jiewen, Z., Jiyong, S., Zhihua, L., & Tingting, S. (2015). Monitoring the biogenic amines in Chinese traditional salted pork in jelly (Yao-meat) by colorimetric sensor

array based on nine natural pigments. *International Journal of Food Science & Technology, 50*(1), 203-209.

Xu, Y. X., Kim, K. M., Hanna, M. A., & Nag, D. (2005). Chitosan–starch composite film: preparation and characterization. *Industrial Crops and Products, 21*(2), 185-192.

Yoon, S.-D., Chough, S.-H., & Park, H.-R. (2006). Effects of additives with different functional groups on the physical properties of starch/PVA blend film. *Journal of Applied Polymer Science, 100*(5), 3733-3740.

Zhang, X., Lu, S., & Chen, X. (2014). A visual pH sensing film using natural dyes from Bauhinia blakeana Dunn. *Sensors and Actuators B: Chemical, 198*, 268-273.

Zhang, X., Sun, G., Xiao, X., Liu, Y., & Zheng, X. (2016). Application of microbial TTIs as smart label for food quality: Response mechanism, application and research trends. *Trends in Food Science & Technology, 51*, 12-23.

Figure captions

Fig. 1. (a) Color and (b) UV-vis spectra of RACNs solution (0.12 mg/mL) at pH 2-12.

Fig. 2. FTIR spectra of (a) starch, (b) PVA, (c) RACNs, (d) SPVA film, (e) SPVA/RACNs-30 film, (f) SPVA/RACNs-60 film and (g) SPVA/RACNs-120 film.

Fig. 3. XRD spectra of starch, PVA, SPVA film, SPVA/RACNs-30 film, SPVA/RACNs-60 film and SPVA/ RACNs-120 film.

Fig. 4. SEM micrographs of the cross sections of (a) SPVA film, (b) SPVA/RACNs-30 film, (c) SPVA/RACNs-60 film, and (d) SPVA/RACNs-120 film.

Fig. 5. The relative color change (*S*) of the colorimetric films stored at 4℃ and 25℃ for 14 d.

Fig. 6. UV-vis spectra of (a) SPVA/RACNs-30 film, (b) SPVA/RACNs-60 film and (c) SPVA/RACNs-120 film when exposed to ammonia generated from a 8 mM ammonia solution at 25℃ for 24 min, and (d) the change of the absorbance ratio at 640 nm versus 540 nm (A_{640}/A_{540}).

Fig. 7. (a) The change of TVB-N level of stored silver carp within 165 h at 4℃ and (b) the corresponding color changes of the colorimetric films.

Fig. 1

(a)

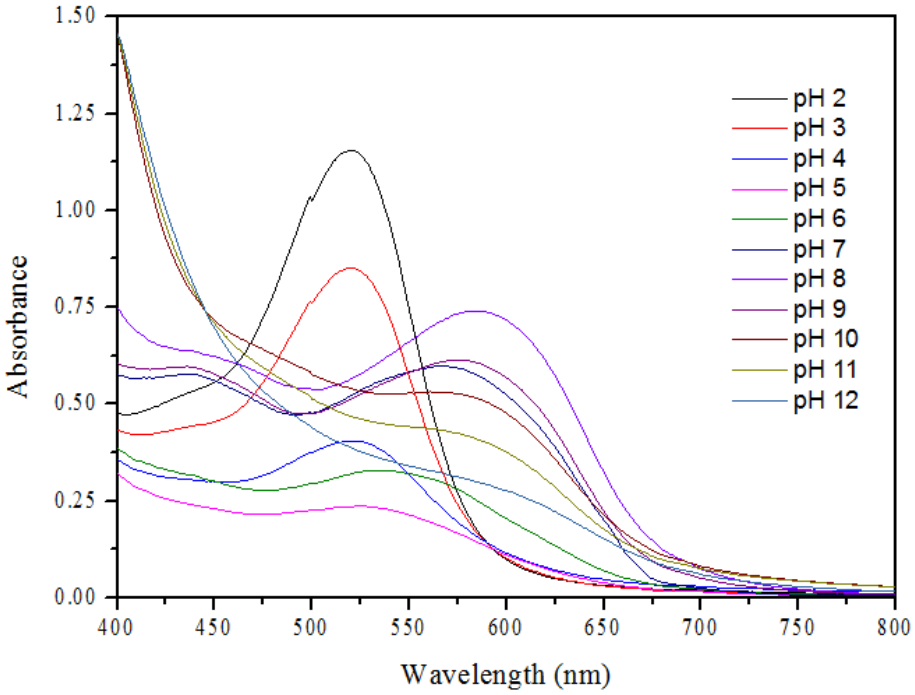

(b)

Fig. 2

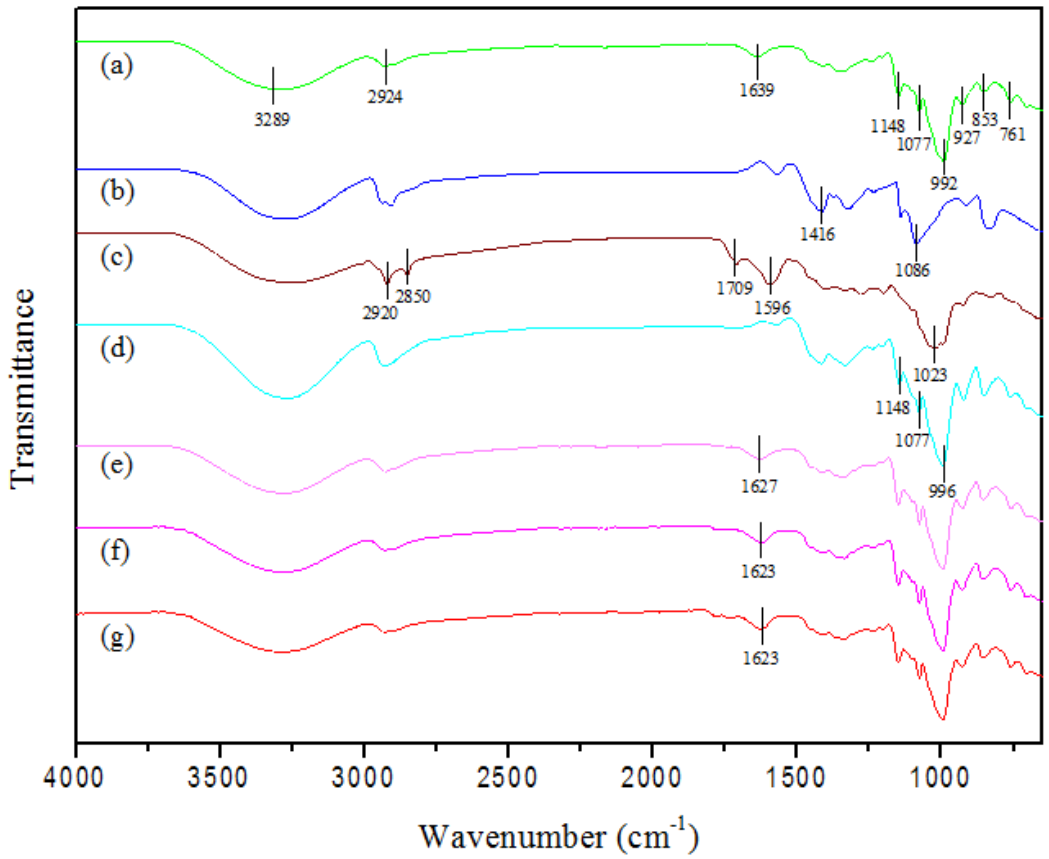

Fig. 3 revision FOOHYD 3804

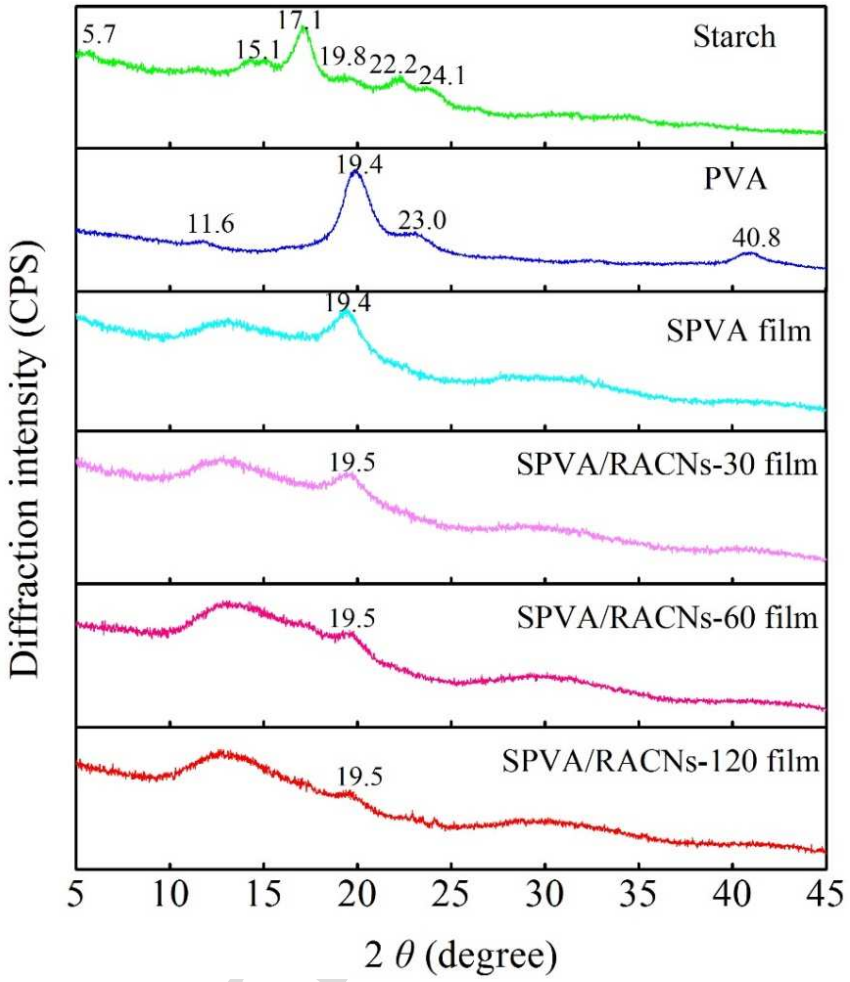

Fig. 4

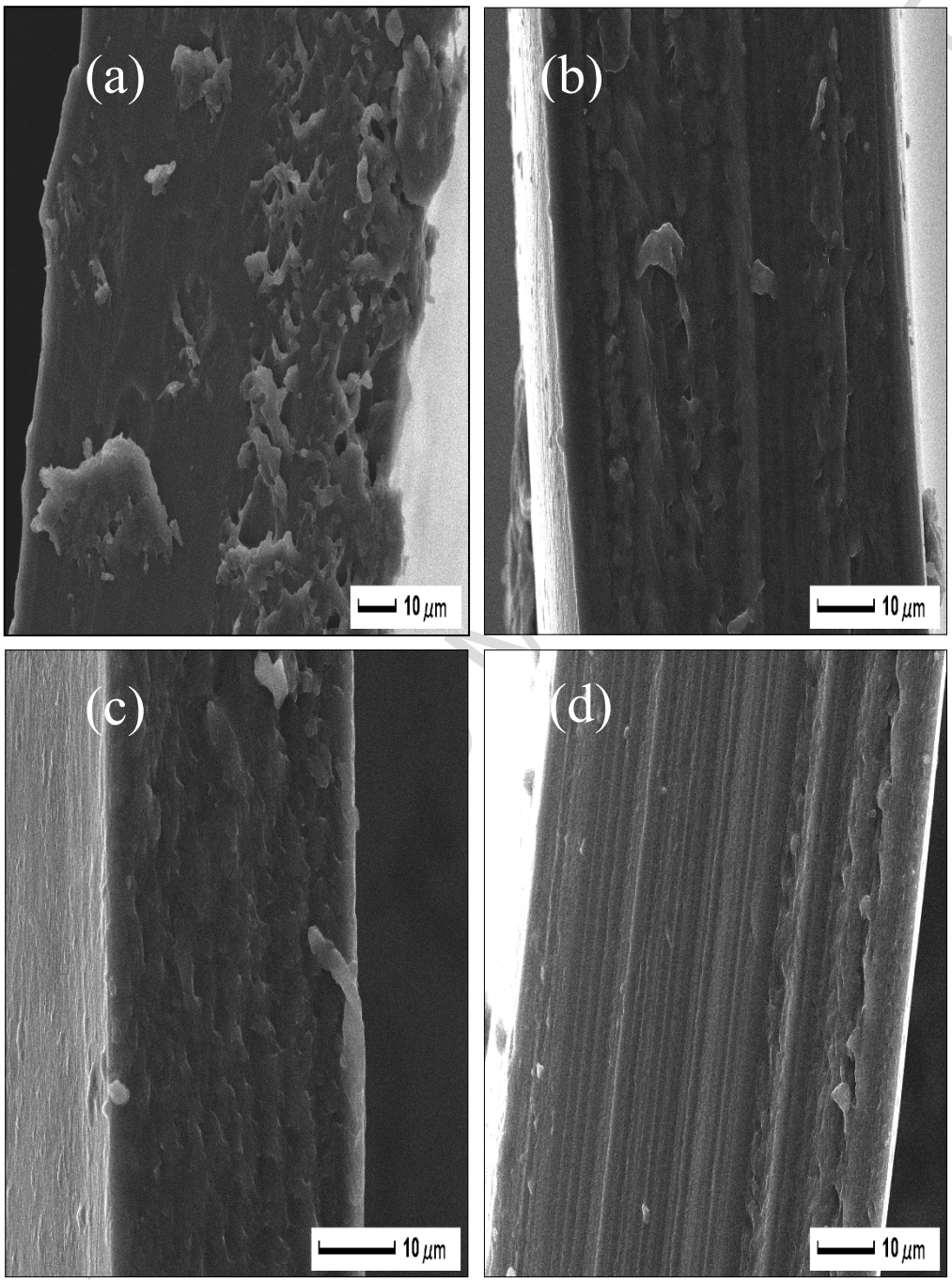

Fig. 5

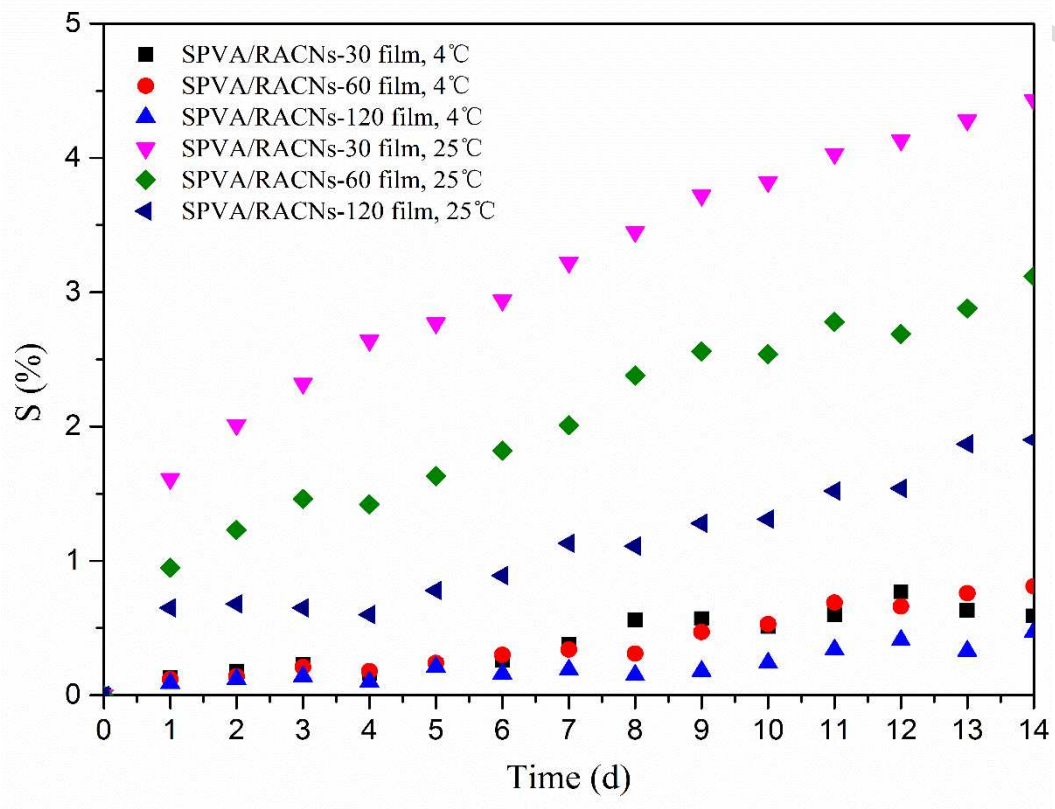

Fig. 6

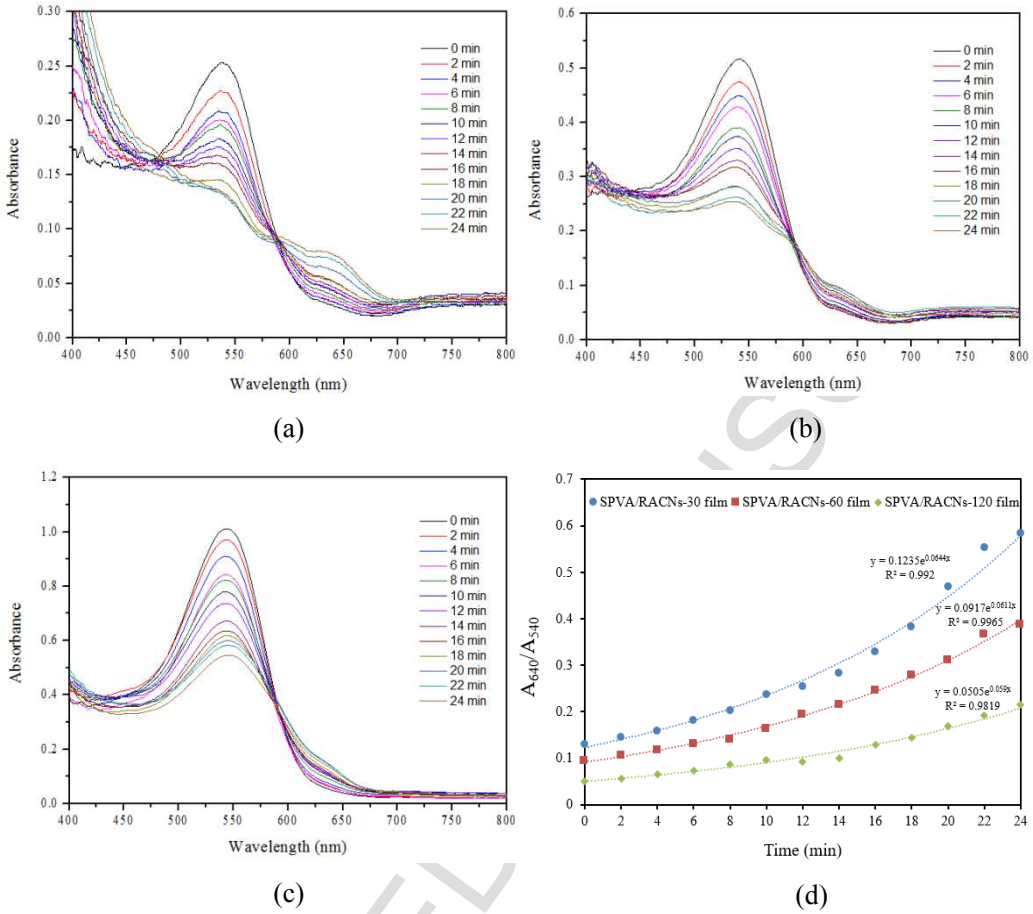

Fig. 7

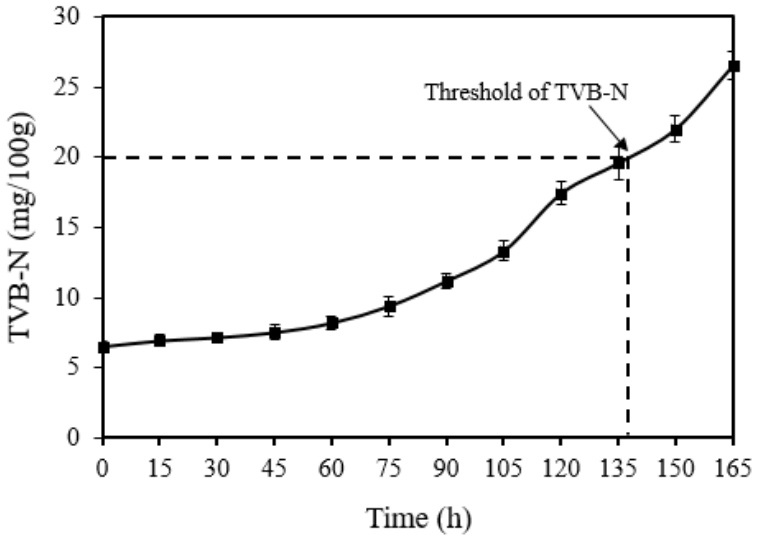

(a)

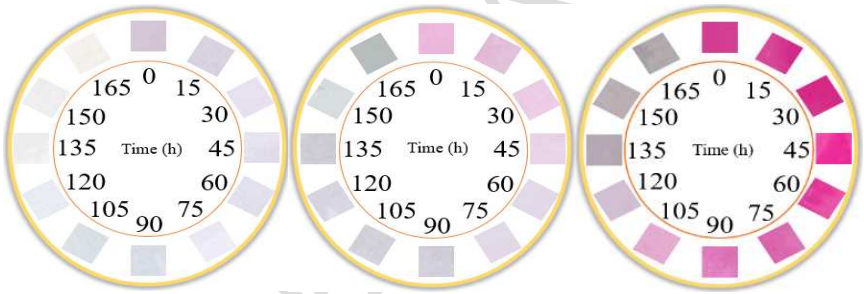

SPVA/RACNs-30 film SPVA/RACNs-60 film SPVA/RACNs-120 film

(b)

Table 1

Thickness, water content, tensile strength and elongation at break of the SPVA film and the colorimetric films.

Films	Thickness (μm)	Water content (%)	Tensile strength (MPa)	Elongation at break (%)
SPVA	88.06 ± 3.10^{b}	25.50 ± 0.98^{a}	48.97 ± 2.36^{a}	44.15 ± 2.42^{d}
SPVA/RACNs-30	88.40 ± 3.21^{b}	25.21 ± 1.47^{a}	48.21 ± 2.60^{a}	49.12 ± 2.09^{c}
SPVA/RACNs-60	89.25 ± 2.57^{b}	22.04 ± 1.33^{b}	45.17 ± 1.78^{b}	60.24 ± 3.18^{b}
SPVA/RACNs-120	93.89 ± 3.13^{a}	18.50 ± 0.98^{c}	41.85 ± 2.03^{c}	88.28 ± 3.51^{a}

Data were presented as mean ± standard deviation of three samples.

Data in the same column with different letter were significantly different ($p < 0.05$).